ARTICLE

Solvent Reorganization Energy and Electronic Coupling for Intramolecular Electron Transfer in Biphenyl-Acceptor Anion Radicals

Jing-bo Wang[a,b], Jian-yi Ma[a,b], Xiang-yuan Li[a,b*], Fu-cheng He[a], Ke-xiang Fu[a]

a. College of Chemical Engineering, Sichuan University, Chengdu 610065, China;
b. Institute for Nanobiomedical Technology and Membrane Biology, Sichuan University, Chengdu 610065, China

(Dated: Received on March 23, 2007; Accepted on March 24, 2007)

A novel algorithm was designed and implemented to realize the numerical calculation of the solvent reorganization energy for electron transfer reactions, on the basis of nonequilibrium solvation theory and the dielectric polarizable continuum model. Applying the procedure to the well-investigated intramolecular electron transfer in biphenyl-androstane-naphthyl and biphenyl-androstane-phenanthryl systems, the numerical results of solvent reorganization energy were determined to be around 60 kJ/mol, in good agreement with experimental data. Koopman's theorem was adopted for the calculation of the electron transfer coupling element, associated with the linear reaction coordinate approximation. The values for this quantity obtained are acceptable when compared with experimental results.

Key words: Nonequilibrium salvation, Electron transfer, Solvent reorganization energy, Continuum model

I. INTRODUCTION

There has been a long-standing interest in nonequilibrium solvation processes. Nonequilibrium solvation is important to describe many chemical processes in solution such as electron transfer (ET), photoionization, and light absorption/emission [1-5]. In nonadiabatic ET processes, the reorganization energy λ is one of the key quantities that control the reaction rate. λ consists of two parts: solvent reorganization energy, λ_s, and inner reorganization energy, λ_{in}. Marcus' two-sphere model [6] provides an excellent tool for the estimation of λ_s, but the theoretical predictions in some cases are substantially overestimated when compared with those evaluated from experimental fittings [7-10]. The most remarkable example is the predictions for Closs-Miller experiments [11-14]. Therefore, instead of the two-sphere model which often fails in accurately describing experimental results, the λ_s values are derived from a combination of theory and experiment [15].

In the exploration of long-range ET processes, molecules with the topology of donor-spacer-acceptor are playing a central role in the investigation of the rate of ET. One of the best experiments was provided in 1984 by Miller and Closs [11]. They investigated compounds in which 4-biphenyl group was connected via a rigid spacer to various acceptor groups. Biphenyl-androstane-naphthyl (denoted as Bp-spacer-Np) and biphenyl-androstane-phenanthryl (Bp-spacer-Ph) systems are two model molecules adopted in the well-known Closs-Miller experiments. In these model systems, the 5-α-androstane skeleton is a rigid saturated hydrocarbon spacer without electron affinity. 4-biphenyl substitutes at 16-β and 2-naphthyl as well as 9-phenanthryl attach at position 3 with β stereochemistry [12]. An extra electron transfers from the 4-biphenyl radical anion to the acceptor, 2-naphthyl or 9-phenanthryl (Scheme 1).

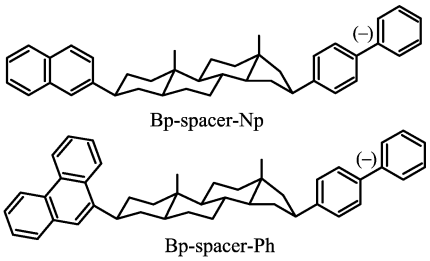

Scheme 1

The ET rates from biphenyl to various acceptors were measured. Using plots of ET rate constants versus driving force, through Marcus normal and inverted regions, Closs and Miller obtained useful estimations of λ_s and λ_{in}. They are 59.82 kJ/mol (0.62 eV) and 55.96 kJ/mol (0.58 eV) respectively for the two systems, excluding the contribution of 12.5 kJ/mol from the low frequency rotation motion around the C−C bond between the two benzene rings of a biphenyl group [11,12,14]. Here λ_s is considerably smaller than the prediction by the conventional two-sphere model [13,16]. Attempts were made to improve on the poor computational results within the framework of the econtinuum model, but it seems no essential change can be made [13,15,17]. A noteworthy method in recent years is the molecular simulation of λ_s. In this way, part of the system is considered at the molecular level but the rest is treated as a polarizable continuum. Much progress toward molecular level

*Author to whom correspondence should be addressed. E-mail: xyli@scu.edu.cn

descriptions has been reported for studies of both small and large systems [18-21].

In preceding articles, the authors clarified that the conventional theories of nonequilibrium solvation contain some defects, and put forward a new set of formulations [22-26]. The motivation of this work is to apply the newly developed procedure to solve the problem of the discrepancy between the theoretical predication and the well-done experimental fittings. In this paper, the new formulations on nonequilibrium theories developed most recently are briefly introduced, and the new expression of λ_s is deduced. Secondly, among the several polarizable continuum models [27-30], the dielectric polarizable continuum model (D-PCM) is adopted to realize the numerical calculation for solving the Poisson equation and for determining the polarization surface charges, employing the Gamess package [31,32] to which some subroutines were added by the authors in order to realize the solvation energy calculation of the nonequilibrium state. We call the procedure combining the nonequilibrium solvation and the popular D-PCM the nonequilibrium polarizable continuum model (N-PCM). Consequently the equilibrium and nonequilibrium solvation energies were calculated. The modified program was applied to the molecular systems Bp-spacer-Np and Bp-spacer-Ph. Through comparison, it is found that the numerical results match the experimental values very well.

II. BASIC FORMULATIONS

A. New expression for solvent reorganization energy

The solvent reorganization energy is a dominating quantity in ET. In order to derive it, we at first present the electrostatic free energies in both equilibrium and nonequilibrium states, within the framework of the continuum model. Let us consider a process of ET for a molecule in solution. At the equilibrium state, the solute-solvent system reaches the polarization equilibrium. The electrostatic free energy is well known as [33]

$$G_1^{\rm eq} = \frac{1}{2}\int_V \rho_1 \phi_1^{\rm eq} {\rm d}V \tag{1}$$

where "1" refers to the initial state and "eq" to the equilibrium. Throughout this work we use ρ to denote the continuous distribution of the solute charge, distinguishing it from the discrete charges $Q(i)$ of the solute that appear in the following sections. $\phi_1^{\rm eq}$ stands for the total equilibrium potential in the medium with a static dielectric constant of $\varepsilon_{\rm s}$ and it includes two parts: the vacuum potential ψ_1 of the solute and the equilibrium polarization potential $\varphi_1^{\rm eq}$ due to the solvent response. Cutting off the self-energy of the solute charge, say, $\frac{1}{2}\int_V \rho_1\psi_1 {\rm d}V$, the equilibrium solvation energy is given by

$$\Delta F_1^{\rm eq} = \frac{1}{2}\int_V \rho_1 \varphi_1^{\rm eq} {\rm d}V \tag{2}$$

In an ET process, the solute is supposed to undergo a sudden change of charge density to ρ_2, but only the electronic polarization of the solvent, corresponding to the medium of $\varepsilon_{\rm op}$, responds to the change of solute charge. Here $\varepsilon_{\rm op}$ represents the optical dielectric constant. In the most recent work by the authors [22-26], several approaches to the expression of the nonequilibrium solvation energy have been presented, among which the most straightforward one is the field superposition principle. A brief derivation for electrostatic free energy of nonequilibrium through the field superposition approach is given as follows.

The nonequilibrium state $[\rho_2, {\phi_2}^{\rm non}]$ can be thought as a superposition of the two independent equilibrium states $[\rho_2, {\phi_2}^{\rm eq}]$ and $[\Delta\rho, \Delta\phi_{\rm op}]$ which respectively relate to the polarization equilibrium corresponding to ρ_1 in the realistic medium of $\varepsilon_{\rm s}$, and the polarization equilibrium of $\Delta\rho$ in the hypothetical medium of $\varepsilon_{\rm op}$. $\Delta\phi_{\rm op}$ is the potential change resulting from $\Delta\rho$ in the medium of $\varepsilon_{\rm op}$. According to the superposition principle, the total free energy consists of three constituents: the individual energies of the two fields, and the interaction energy between them [23,24,26]. In other words,

$$G_2^{\rm non} = \frac{1}{2}\int_V \rho_1\phi_1^{\rm eq}{\rm d}V + \frac{1}{2}\int_V \Delta\rho\Delta\phi_{\rm op}{\rm d}V + \frac{1}{2}\int_V (\rho_1\Delta\phi_{\rm op} + \Delta\rho\phi_1^{\rm eq}){\rm d}V \tag{3}$$

here the subscript "2" and the superscript "non" refer to the final nonequilibrium state. Noting that $\Delta\rho{=}\rho_2{-}\rho_1$, and the $\phi_2^{\rm non}$ is the sum of $\phi_1^{\rm eq}$ and $\Delta\phi_{\rm op}$, Eq.(3) becomes

$$G_2^{\rm non} = \frac{1}{2}\int_V \rho_2\phi_2^{\rm non}{\rm d}V \tag{4}$$

For this expression, a more general derivation invoking the principle of thermodynamics with the reversible work is given in the appendix. The expression of $G_2^{\rm non}$ is different from the traditional Marcus expression [34-36]. The nonequilibrium potential $\phi_2^{\rm non}$ can be decomposed into two parts, the vacuum potential ψ_2 due to ρ_2 in vacuum and the nonequilibrium polarization potential $\phi_2^{\rm non}$ caused by the nonequilibrium response of the solvent. Similar to Eq.(2), the nonequilibrium solvation energy is thus given by

$$\Delta F_2^{\rm non} = \frac{1}{2}\int_V \rho_2\varphi_2^{\rm non}{\rm dV} \tag{5}$$

Concerning $\lambda_{\rm s}$ of ET, we define the solvent reorganization energy as the difference of the salvation free energies between the nonequilibrium and equilibrium states

DOI:10.1088/1674-0068/21/01/45-54

with respect to the same solute charge. Thus, the solvent reorganization energy of ET can be expressed as

$$\lambda_{\rm bw} = \Delta F_2^{\rm non} - \Delta F_2^{\rm eq} \tag{6}$$

where the subscript "bw" refers to ET that we call the "backward ET". Substituting the expressions of $\Delta F_2^{\rm non}$ and $\Delta F_2^{\rm eq}$ into Eq.(6), we obtain

$$\lambda_{\rm bw} = \frac{1}{2}\int_V \rho_2(\varphi_2^{\rm non} - \varphi_2^{\rm eq}){\rm d}V \tag{7}$$

With the two equalities $\Delta\varphi_{\rm op}$=$\varphi_2^{\rm non}$−$\varphi_1^{\rm eq}$ and $\Delta\varphi_{\rm s}$=$\varphi_2^{\rm eq}$−$\varphi_1^{\rm eq}$, the final expression of $\lambda_{\rm bw}$ is as follows,

$$\lambda_{\rm bw} = \frac{1}{2}\int_V \rho_2(\Delta\varphi_{\rm op} - \Delta\varphi_{\rm s}){\rm d}V \tag{8}$$

here $\Delta\varphi_{\rm s}$ can be thought as the difference of equilibrium polarization potentials caused by ρ_2 and ρ_1 in the medium of $\varepsilon_{\rm s}$. $\Delta\varphi_{\rm op}$ is the change of polarization potential due to $\Delta\rho$ in the hypothetical medium of $\varepsilon_{\rm op}$.

Parallel derivations can be applied to the "forward ET" and $\lambda_{\rm fw}$ is thus given by,

$$\begin{aligned}\lambda_{\rm fw} &= \Delta F_1^{\rm non} - \Delta F_1^{\rm eq} \\ &= \frac{1}{2}\int_V \rho_1(\Delta\varphi_{\rm s} - \Delta\varphi_{\rm op}){\rm d}V \end{aligned}\tag{9}$$

Comparing Eqs.(8) and (9), the derivation reveals a remarkable feature that the solvent reorganization energy with different definitions, Eqs.(6) and (9), are different in general, unlike the theoretical models developed previously that give an identical result for both definitions [35,36]. According to the derivations presented here, the average value of $\lambda_{\rm fw}$ and $\lambda_{\rm bw}$ is given by [23-25]

$$\begin{aligned}\lambda_{\rm s} &= \frac{1}{2}(\lambda_{\rm fw} + \lambda_{\rm bw}) \\ &= \frac{1}{4}\int_V \Delta\rho(\Delta\varphi_{\rm op} - \Delta\varphi_{\rm s}){\rm d}V \end{aligned}\tag{10}$$

If we compare the current result with the earlier developed ones by other authors [16,35,36], it is easy to see that the conventional models overestimate the solvent reorganization energy by a factor of 2. This comparison gives a satisfactory explanation for the failure of the earlier theoretical models in predicting the solvent reorganization energies [10,14,16].

In the following paragraphs, the implementation of numerical calculation with the modified Gamess package is discussed. A practical expression of $\lambda_{\rm s}$ for numerical calculation is

$$\lambda_{\rm s} = \frac{1}{2}(\Delta F_2^{\rm non} - \Delta F_2^{\rm eq} + \Delta F_1^{\rm non} - \Delta F_1^{\rm eq}) \tag{11}$$

As shown in Eq.(11), the four solvation energies need to be calculated. Scheme 2 shows the method used to obtain the total energy and the polarization charges with discrete form [24]. Here we use U to denote the total energy after self consistent reaction field (SCRF) treatment for a specific state. The corresponding solvation energy can be obtained by cutting the vacuum energy from the total energy. $\{Q(i)\}$ stands for the discrete solute charges, and $\{q(i)\}$ the polarization charges. Beginning with this, the explanation below shows how to realize the separation of slow and fast polarization charges and to obtain the total free energy.

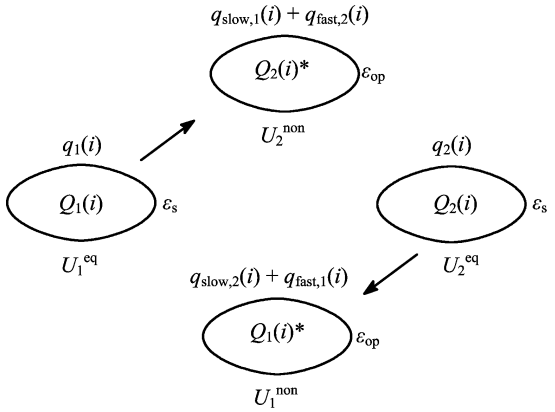

Scheme 2

B. Numerical algorithm

In PCM, the solvent is modeled as a continuous medium, characterized solely by a scalar dielectric constant. The polarization field of the dielectric medium is reduced to the creation of polarization charges on the surface of the cavity containing the solute. In computation practice, the cavity surface is partitioned into small domains, called "tesserae", and the continuous surface charge is cut into a discrete set of point charges lying on the tesserae. In order to obtain the value of discrete point charges, the boundary element equation was established. For the equilibrium state, the matrix equation for the polarization charges is given by

$$\mathbf{D}(\varepsilon_{\rm s})\mathbf{q}_1 = \mathbf{b}_1 \tag{12}$$

where $\mathbf{D}(\varepsilon_{\rm s})$ is the interaction matrix collecting elements related to geometry of the cavity and depends on $\varepsilon_{\rm s}$. $\mathbf{q}_1$ is the set of polarization charges to be solved on the cavity surface, and $\mathbf{b}_1$ is a column vector collecting the normal components of the electric field of the solute at the representative points of each tesserae [37]. The subscript "1" in Eq.(12) indicates the initial equilibrium state. Concrete expressions for matrix elements of $\mathbf{D}$ are [37]

$$D_{ii} = \frac{2\pi}{s_i}\left(\frac{\varepsilon_{\rm s+1}}{\varepsilon_{\rm s}-1} + \sqrt{\frac{s_i}{4\pi {l_i}^2}}\right) \tag{13}$$

DOI:10.1088/1674-0068/21/01/45-54

$$D_{ij} = \frac{(\mathbf{r}_i - \mathbf{r}_j)\cdot\mathbf{n}_i}{|\mathbf{r}_i - \mathbf{r}_j|^3} \qquad (i \neq j) \tag{14}$$

$$b_i = -\sum_k Q(k)\frac{(\mathbf{r}_i - \mathbf{R}_k)\cdot\mathbf{n}_i}{|\mathbf{r}_i - \mathbf{R}_k|^3} \tag{15}$$

where s_i denotes the area of tessera i. Every s_i is replaced by the area of sphere cap i with radius l_i. $\mathbf{r}_i$ and $\mathbf{r}_j$ are the centers of the ith and jth tesserae respectively. $\mathbf{R}_k$ is the coordinate of kth solute charge $Q(k)$ and $\mathbf{n}_i$ stands for the normal vector of the ith tesserae. Once the discrete polarization charges have been determined through Eq.(12), they are used to modify the solute Hamiltonian. Considering the solute-solvent interactions, the perturbation $\mathbf{H}'$ is added to the vacuum Hamiltonian $\mathbf{H}^0$, i.e.

$$\mathbf{H} = \mathbf{H}^0 + \frac{1}{2}\mathbf{H}' \tag{16}$$

$\mathbf{H}'$ represents the potential arising from the discrete polarization charges on the cavity and is defined as [24]

$$\mathbf{H}' = \sum_i \frac{q_1(i)}{|\mathbf{r} - \mathbf{r}_i|} \tag{17}$$

The expectation value of the electron Hamiltonian under the condition of equilibrium polarization, is obtained as

$$w_1^{\rm eq} = \langle\Psi_1^{\rm eq}|\mathbf{H}^0 + \frac{1}{2}\mathbf{H}'|\Psi_1^{\rm eq}\rangle \tag{18}$$

where $\Psi_1^{\rm eq}$ is the electronic wave function of the solute. In this work we use $\mathbf{H}'$ defined in Eq.(17) to construct the Fock operator $\mathbf{F}_i$ in iterative process of self-consistent field. The Hartree-Fock equation is of the following form

$$(\mathbf{F}_i + \mathbf{H}')\phi_i = e_i\phi_i \tag{19}$$

where ϕ_i stands for the molecular orbital in the presence of the reaction field. Consequently the solute wave function is modified by the polarization charges, which in turn depend on the solute charge distribution and the polarization charges. The wave function must be iterated to convergence [24,37]. Finally, the total polarization charges $\mathbf{q}_1$ and solute wave function $\Psi_1^{\rm eq}$ for the equilibrium condition are obtained.

Let us consider a sudden change in the solute charge in ET process at the transition state. The system changes from the equilibrium state 1 to the nonequilibrium state 2. In this case, only the fast component of the polarization charges adjusts itself without time lag to fit with any change in solute charge, while the slow component stays the same due to the solvent inertial polarization [3,37]. Therefore, it is advisable to suppose that the solute is surrounded by the medium of $\varepsilon_{\rm op}$, and the fixed slow component of the polarization charges affects the solute wave function. The fast part of the polarization charges, $\mathbf{q}_{\rm fast,1}$, can be determined through the matrix equation given below [3,37],

$$\mathbf{D}(\varepsilon_{\rm op})\mathbf{q}_{\rm fast,1} = \mathbf{b}_1 \tag{20}$$

In Eq.(20), $\varepsilon_{\rm op}$ is used to replace $\varepsilon_{\rm s}$ in the expression of $\mathbf{D}$, i.e. Eqs.(13)-(15). It should be noted that, $\mathbf{q}_1$ and $\mathbf{q}_{\rm fast,1}$ can be obtained through solving Eqs.(12) and (20) respectively at equilibrium state 1. Consequently, the slow component of polarization charges, $\mathbf{q}_{\rm slow,1}$, is given by

$$\mathbf{q}_{\rm slow,1} = \mathbf{q}_1 - \mathbf{q}_{\rm fast,1} \tag{21}$$

During ET process, the fast component of polarization charges is assumed to equilibrate simultaneously with the new solute wave function $\Psi_2^{\rm non}$ in the medium of $\varepsilon_{\rm op}$, and becomes $\mathbf{q}_{\rm fast,2}$, while the slow charges are the same as in Eq.(21). Of course, both sets of charges perturb the solute wave function. Therefore, the total discrete polarization charges $\mathbf{q}_2^*$ for nonequilibrium state 2 can be written as

$$\mathbf{q}_2^* = \mathbf{q}_{\rm slow,1} + \mathbf{q}_{\rm fast,2} \tag{22}$$

the superscript "*" refers to the nonequilibrium state. It should be mentioned that $\mathbf{q}_2$ and $\mathbf{q}_2^*$ are not the same owing to the different influences from the solvent polarization. From Eq.(17), we can write the perturbation $\mathbf{H}''$ for nonequilibrium in terms of discrete charge as,

$$\mathbf{H}'' = \sum_i \frac{\mathbf{q}_2^*(i)}{|\mathbf{r} - \mathbf{r}_i|} \tag{23}$$

and the expectation value of the electron Hamiltonian in this case is given by

$$w_2^{\rm non} = \langle\Psi_2^{\rm non}|\mathbf{H}^0 + \frac{1}{2}\mathbf{H}''|\Psi_2^{\rm non}\rangle \tag{24}$$

where $\Psi_2^{\rm non}$ denotes the electronic wave function of the solute under the nonequilibrium condition. The corresponding Hartree-Fock equation can be written as

$$(\mathbf{F}_i + \mathbf{H}'')\phi_i = e_i\phi_i \tag{25}$$

Similar to the treatment for equilibrium state, the total polarization charges $\mathbf{q}_2^*$ and the wave function $\Psi_2^{\rm non}$ are also obtained through SCRF treatment.

Based on the authors' previous work [23,24,26], the total energy of the solute in equilibrium state is as

$$U_1^{\rm eq} = \langle\Psi_1^{\rm eq}|\mathbf{H}^0 + \frac{1}{2}\mathbf{H}'|\Psi_1^{\rm eq}\rangle + \frac{1}{2}\sum_i\sum_j \frac{q_1(i)Z_j}{|\mathbf{r}_i - \mathbf{R}_j|} + E_{\rm N} \tag{26}$$

where Z_j is the nuclear core charge at $\mathbf{R}_j$ and the second term represents the interaction between nuclear core charges and the polarization charges, while the sign $E_{\rm N}$

DOI:10.1088/1674-0068/21/01/45-54

stands for the nuclear repulsion energy of the solute. On the other hand, the total energy of the solute in vacuum can be given as

$$U_1^{\rm gas} = \langle \Psi_1^{\rm gas} | \mathbf{H}^0 | \Psi_1^{\rm gas} \rangle + E_{\rm N} \tag{27}$$

where $\Psi_1^{\rm gas}$ is the solute wave function in vacuum. Therefore the solvation energy of the equilibrium condition can be expressed as

$$\begin{aligned} \Delta F_1^{\rm eq} &= U_1^{\rm eq} - U_1^{\rm gas} \\ &= \langle \Psi_1^{\rm eq} | \mathbf{H}^0 + \frac{1}{2}\mathbf{H}' | \Psi_1^{\rm eq} \rangle - \langle \Psi_1^{\rm gas} | \mathbf{H}^0 | \Psi_1^{\rm gas} \rangle \\ &\quad + \frac{1}{2} \sum_i \sum_j \frac{q_1(i) Z_j}{|\mathbf{r}_i - \mathbf{R}_j|} \end{aligned} \tag{28}$$

For nonequilibrium state 2, the total energy of the system is given by

$$\begin{aligned} U_2^{\rm non} &= \langle \Psi_2^{\rm non} | \mathbf{H}^0 + \frac{1}{2}\mathbf{H}'' | \Psi_2^{\rm non} \rangle \\ &\quad + \frac{1}{2} \sum_i \sum_j \frac{q_2^*(i) Z_j}{|\mathbf{r}_i - \mathbf{R}_j|} + E_{\rm N} \end{aligned} \tag{29}$$

Similar to Eq.(27), the total energy of the solute in gas-phase for nonequilibrium state is

$$U_2^{\rm gas} = \langle \Psi_2^{\rm gas} | \mathbf{H}^0 | \Psi_2^{\rm gas} \rangle + E_N \tag{30}$$

Therefore, the solvation energy of the nonequilibrium state can be written as

$$\begin{aligned} \Delta F_2^{\rm non} &= U_2^{\rm non} - U_2^{\rm gas} \\ &= \langle \Psi_2^{\rm non} | \mathbf{H}^0 + \frac{1}{2}\mathbf{H}'' | \Psi_2^{\rm non} \rangle - \langle \Psi_2^{\rm gas} | \mathbf{H}^0 | \Psi_2^{\rm gas} \rangle \\ &\quad + \frac{1}{2} \sum_i \sum_j \frac{q_2^*(i) Z_j}{|\mathbf{r}_i - \mathbf{R}_j|} \end{aligned} \tag{31}$$

It should be mentioned that all the calculations are performed at the transition state configuration, and therefore the nuclear repulsion term of the solute is the same for all four states. Now that the numerical calculation of the solvent reorganization energy has been realized based on these new nonequilibrium formulations within the framework of PCM, we call it N-PCM. A few subroutines have been added to Gamess for our purposes.

III. RESULTS AND DISCUSSION

The rigid spacer mediated ET reactions between biphenyl anion radical and different acceptors were intensively investigated by Closs and Miller. Plots of ET rate constants versus driving force provided useful fitting values of $\lambda_{\rm s}$, $\lambda_{\rm in}$ and the electronic coupling matrix element $V_{\rm DA}$, based on the semi-classical ET model [11-14]. In the fitting procedure, several tacit assumptions were invoked. Among them, the one is the treatment of the whole series of molecules with invariant reorganization energies, $\lambda_{\rm s}$ and $\lambda_{\rm in}$. Another assumption is that $V_{\rm DA}$ can be treated as a constant throughout the series [12]. Hence some authors began to doubt the reliability of the experimental values after several attempts [17,19,21]. Note also that some authors developed perturbation molecular orbital theory [36] which treats the $V_{\rm DA}$ as a variable to fit the ET rates obtained by Closs and Miller, and therefore obtained different values for $\lambda_{\rm s}$ and $\lambda_{\rm in}$. In this work, the original fitting parameters are adopted as the experimental values. Although we cannot definitely confirm the accuracy of experimental values, the theoretical results of this work show a good consistency between our theory and the experimental fittings for the parameters of $\lambda_{\rm s}$, $\lambda_{\rm in}$, and $V_{\rm DA}$.

In the following parts, the computation details of Bp-spacer-Np system are illustrated, and the Bp-spacer-Ph system is treated in a similar way.

A. Electron localized state

In computing the parameters mentioned above, the reactant and the product geometries for the intramolecular ET were prepared as a first step. For the purpose of electron-localization on different sites, we wish to find the geometries of the whole system in which an extra electron almost entirely localizes either at the donor site (reactant) or the acceptor site (product). From the experience of the authors [39], the isolate optimized anion geometry of the donor and the neutral structure of the acceptor can guarantee the electron localization of the reactant system, provided that the donor and the acceptor do not considerably differ from each other in electronegativity, as in the case of biphenyl and naphthyl. The structures of the four species for the donor and acceptor, i.e., the biphenyl anion, Bp^-, the naphthalene anion, Np^-, the neutral biphenyl, Bp, and the neutral naphthalene, Np, are optimized at the HF/6-31G** level. Here we choose a comparatively lower basis level in order to match the further calculations of the donor-spacer-acceptor system. Furthermore, we need the structure of the spacer that is assumed rigid during the ET process. Considering the conformation of the whole system, the neutral molecular system Bp-spacer-Np is optimized at the HF/6-31G level, and then the separately optimized donor anion Bp is used to replace the biphenyl fragment of neutral Bp-spacer-Np system. In a parallel way, the separately optimized neutral acceptor Np is used to replace the acceptor part in the neutral Bp-spacer-Np system. During the linkage, the orientations of the donor and the acceptor with respect to the spacer remain, and also the lengths of the C−C bond that connects the donor or the acceptor to the spacer. At this stage, the structure of the reactant for intramolecular ET has been prepared. The same strategy is also valid for the preparation of the product geometry. The geometries of the reactant and the product

DOI:10.1088/1674-0068/21/01/45-54

prepared in this way are respectively denoted as Bp^--spacer-Np and Bp-spacer-Np^-. They are assumed to be the desirable approximations for the optimal geometries of electronically localized states. Further geometrical optimization is not permitted, because of the gain of the electron-localization features. Geometrical optimization confirms that the donor varies from the coplanar anion radical, Bp^- to a twisted neutral biphenyl, Bp, with a torsion angle of 45.5°.

Based on the prepared geometries Bp^--spacer-Np and Bp-spacer-Np^-, the single Slater determinant is constructed and this determinant displays the feature of the localization of an extra electron on either donor or acceptor sites. The net charges both on the donor (reactant) and acceptor (product) exceed −0.90 by Mulliken population analysis. This implies the successful localization of the extra electron. In this way, two sets of molecular orbitals that produce the different electron-localized states are obtained. They are used to maintain the electronic structure of transition state configuration when determining λ_s. Such a technique is called the initial-guess-induced SCF technique [39,40].

In order to evaluate the quantity of transferred charges, we define a factor η,

$$\eta = \frac{1}{2}(P_{\rm D}^{\rm p} - P_{\rm D}^{\rm r} + P_{\rm A}^{\rm p} - P_{\rm A}^{\rm r}) \tag{32}$$

here P is the Mulliken population for both the donor fragment and the acceptor one. In this treatment, P is simply a sum of the net charges brought by the specified species. The superscripts "r" and "p" refer to the states of reactant and product respectively. Note that η<1 means a partial ET.

B. Inner reorganization energy

$\lambda_{\rm in}$ corresponds to the energy required to accommodate the nuclear rearrangements occurring upon ET when going from the optimal geometry of initial state to that of the final state. Several methods can provide an estimation of $\lambda_{\rm in}$ [2,25,41,42]: one is based on frequency analysis, the second is based on the energy curves of charge-localized states which is difficult to apply to the large molecules, and the third is to take only the isolated donor and acceptor into account. The androstane skeleton is rigid, so it is reasonable to assume a fixed geometry for the spacer, and thus the third method serves our purpose. In this work, $\lambda_{\rm in}$ is approximated as the average of the following two self-exchange ET reactions. Taking the system Bp-spacer-Np as example, we have

$$Bp^- + Bp \longrightarrow Bp + Bp^- \tag{33}$$

$$Np^- + Np \longrightarrow Np + Np^- \tag{34}$$

First of all, we obtain the total energies of corresponding optimal energies $E(Bp^-)$ and $E(Bp)$ through single point calculations. On the other hand, we also calculate the energy $E'(Bp^-)$ at the optimal geometry of Bp and $E'(Bp)$ at the optimal geometry of Bp^-. Parallel calculations for Eq.(34) can be made. The inner reorganization energy is thus written as the average value of the two self-exchange reactions, i.e.

$$\lambda_{\rm in} = \frac{1}{2}[E'(Bp^-) + E'(Np) + E'(Np^-) + E'(Bp) - E(Bp) - E(Np^-) - E(Np) - E(Bp^-)] \tag{35}$$

For the purpose of $\lambda_{\rm in}$ calculation, a higher level, DFT-B3LYP/6-31++G**, was adopted to perform the geometrical optimization and the single point calculation for the individual species involved in Eqs.(33) and (34). For the Bp-spacer-Np system, the contribution of the biphenyl group to λ_s was found to be 33.75 kJ/mol and the naphthalene contributes a portion of 17.05 kJ/mol, resulting in 50.80 kJ/mol in total. For the Bp-spacer-Ph system, $\lambda_{\rm in}$ was about 54.71 kJ/mol. These values of inner reorganization energies are in good agreement with the experimental estimation of 55.96 kJ/mol with the low frequency contribution from the rotation around the C−C bond in phenyl group included [11,12,14].

C. Electronic coupling

For a nonadiabatic ET, $V_{\rm DA}$ measures the strength of interaction between charge-localized states of the reactant and the product. A correct calculation of values of $V_{\rm DA}$ is crucial in understanding the reaction type. Several theoretical methods can be used to calculate $V_{\rm DA}$, such as the partition method [43], the variational principle on the basis of two-state approach [40], and Koopmans' theorem (KT) [2,39,44,45]. In applying the two-state model under the framework of nonadiabatic ET, two charge-localized states need to be calculated at the nuclear configuration of transition state first, so the accurate method is difficult to apply to large molecules. Owing to the importance of the transition state, we need to find a way to determine its configuration for the ET system. In doing this, a technique based on KT [39,44,45] is exploited. Although the KT approach works badly in estimating $V_{\rm DA}$ for a short range ET, it works well in the case of long-distance ET [44]. In the KT approach, the value of $V_{\rm DA}$ for an anion system is simply approximated as one half of the energy gap between the lowest unoccupied molecular orbital (LOMO) and the next lowest unoccupied molecular orbital (abbreviated as LOMO+1) of the neutral molecule at the transition state. The geometry of the transition state of ET can be found along an appropriate reaction path by searching for the minimal energy gap between LUMO and LUMO+1 for the neutral system. Thus the electronic coupling is given as one half of the eigenvalue difference of LUMO and LUMO+1 at the transition state configuration

$$V_{\rm DA} = \frac{1}{2}(e_{\rm LUMO+1} - e_{\rm LUMO}) \tag{36}$$

DOI:10.1088/1674-0068/21/01/45-54

Because the accurate determination of the ET reaction path for an even small system is not practicable at present, we apply the linear reaction coordinate R to describe the nuclear configuration variation during ET [40,44]. The nuclear rearrangement along the R can be expressed as

$$C_i = (1-R)C_i^{\mathrm{r}} + RC_i^{\mathrm{p}} \tag{37}$$

where C_i^{r} and C_i^{p} refer to the ith internal nuclear coordinate at the geometries of reactant and product respectively. C_i represents the ith coordinate varying along R. R=0 corresponds to the starting geometries of Bp^--spacer-Np and R=1 to that of Bp-spacer-Np^-. How to select the $3N-6$ independent internal coordinate out of the $3N$ coordinates is somewhat arbitrary, but in the experience of the authors the choice has little influence on the results.

Employing the KT approach, together with the linear reaction coordinate method, a series of eigenvalue gaps was calculated between LUMO and LUMO+1 of the neutral system Bp-spacer-Np along the reaction coordinate R. The results are given in Fig.1. The energy gap minimum, which is presumed to correspond to the nuclear configuration of the transition state of ET, was found at R=0.399 and R=0.410 for Bp-spacer-Np and Bp-spacer-Ph respectively. In Eq.(37), we can determine the geometry of transition state by setting R=0.399 and R=0.410, and consequently all the internal nuclear coordinates of the transition state can be determined. In this way, the values of V_{DA} were determined to be 0.137 and 0.196 kJ/mol for Bp-spacer-Np and Bp-spacer-Ph respectively. The computed V_{DA} values are larger than the experimental estimate, 74 J/mol (6.2 cm^{-1}) [12]. However, the data we refer to as the "experimental" are not a result of explicit experiments,

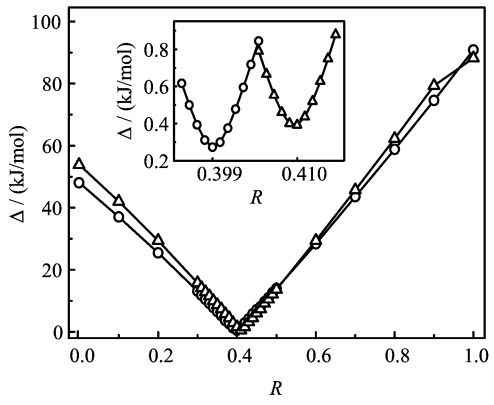

FIG. 1 The energy gap, which is denoted as Δ (Δ= $e_{\mathrm{LUMO+1}}-e_{\mathrm{LUMO}}$). The open circles and open triangles represent the results of Bp-spacer-Np and Bp-spacer-Ph, respectively. R varies from 0 (reactant) to 1 (product). In the range of 0.3-0.5, the step length is 0.01. In the upper panel, R varies from 0.395 to 0.405 for Bp-spacer-Np and from 0.405 to 0.415 for Bp-spacer-Ph and with a step length of 0.001.

being derived from experimental observations after invoking several assumptions. An approximate Golden Rule relationship between the logarithm of the ET constant and the corresponding driving force was applied [12,13] to a series of ET substrates with the same donor (biphenyl) and the same spacer, whereas the acceptor fragment was varied. The reorganization energy and the electronic coupling were taken to be the same for different ET systems. Considering these factors, we should consider the present values of electronic coupling to agree quite well with the experimental fittings. This work shows evidence of the reliability of Koopmans theorem in calculating the elctronic coupling in ET.

D. Solvent reorganization energy

The N-PCM procedure was applied to realize the numerical calculation of λ_{s} for the model systems in 2-methyltetrahydrofuran (MTHF, ε_{s}=6.97, $\varepsilon_{\mathrm{op}}$=1.978). Some new subroutines were added to the Gamess package. The two sets of electron-localized molecular orbitals of Bp^--spacer-Np and Bp-spacer-Np^- were taken as initial guesses to induce the UHF-SCRF calculations at the transition states (R=0.399), using the 6-31G** basis set. The total energies of the four solvation states (see Scheme 2), U_1^{non}, U_2^{eq}, U_2^{non}, and U_1^{eq}, were obtained by SCRF calculations and then the solvation free energy were directly obtained according to Eqs.(28) and (31).

In the framework of PCM, the solute cavity is built with interlocking spheres following the GEPOL procedure [46,47]. The solvent accessible surface is formed starting from van der Waals atomic radii scaled by a factor κ [19,46]. The value of κ is usually assumed the same for all atoms, and the most popular choice for atoms is typically 1.2 [1,3] for this value reproduces the thermochemical data in most cases. Adopting this scaling factor to build the solvent accessible surface, the numerical calculations give the solvation energy for the states depicted in Scheme 2. These energies are displayed in Table I.

Applying Eq.(11), and performing the SCRF calculation, the values of 48.78 and 44.54 kJ/mol for λ_{s} were thus obtained for the systems Bp-spacer-Np and Bp-spacer-Ph respectively. A matter of particular importance is how many charges transferred in computation. According to the definition of η, the values of η obtained were 0.89 for Bp-spacer-Np and 0.88 for Bp-spacer-Ph. The results mean that less than one unit of charge transfers owing to the limitation of the charge localization. In order to do comparison with experimental observations, we need to consider the efficiency of the charge localization and then make some correction so as to fit the actual situation of the whole ET in experiment. To get an approximation, the two-sphere model for λ_{s} can be used. As described in the authors' previous work [22-26], λ_{s} is proportional to the square

DOI:10.1088/1674-0068/21/01/45-54

TABLE I Solvation energy for four solvent states and the solvent reorganization energy (in kJ/mol)

Systems	$\Delta F_1^{\rm eq}$	$\Delta F_2^{\rm non}$	$\Delta F_2^{\rm eq}$	$\Delta F_1^{\rm non}$	$\lambda_{\rm s}({\rm scrf})^{\rm a}$	$\lambda_{\rm s}({\rm corr})^{\rm b}$
Bp-spacer-Np	−187.44	−143.87	−194.07	−140.08	48.78	61.28
Bp-spacer-Ph	−188.23	−141.11	−183.90	−141.94	44.54	57.55

[a] SCRF result of $\lambda_{\rm s}$ by N-PCM, without correction.
[b] $\lambda_{\rm s}$ corrected by the amount of transferred charge, $\lambda_{\rm s}({\rm corr})=\lambda_{\rm s}({\rm scrf})/\eta^2$ (see the text).

of the charge transferred. Therefore, these results can be calibrated to a unit ET by multiplying the SCRF result by a factor of $1/\eta^2$. Hence, the corrected values of $\lambda_{\rm s}$ can be obtained. The results were 61.28 kJ/mol for Bp-spacer-Np and 57.55 kJ/mol for Bp-spacer-Ph. Comparing the present results with the experimental value 59.82 kJ/mol [11,12,14], the values obtained in this work are in perfect agreement with the experimental fittings. The present results show that the N-PCM model behaves well for nonequilibrium solvation. The discrepancies between theoretical predications and experimental fittings in literature can be explained.

As demonstrated in many previous papers, PCM is typically based on the adjustable cavity parameterization. Therefore the impact of scaling factor on numerical calculation is worthy of investigation. Figure 2 illustrates the results. The two curves show a smooth decrease of $\lambda_{\rm s}$ when κ increases. The modest decrease shows that $\lambda_{\rm s}$ is not very sensitive to the choice of κ within an appropriate range.

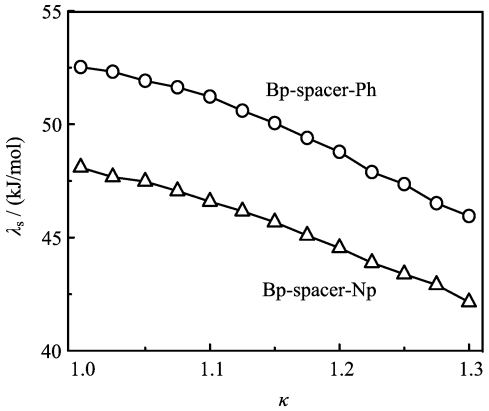

FIG. 2 Influence of scaling factor κ upon $\lambda_{\rm s}$. κ varies from 1.0 to 1.3, and the steplength is 0.025. The open circles and the open triangles represent the results of Bp-spacer-Np and Bp-spacer-Ph respectively.

IV. CONCLUSION

In the present work, a new expression for the electrostatic free energy of nonequlibrium state is put forward, based on the continuum medium theory. Eq.(4) shows that $G_2^{\rm non}$ depends only on the relevant quantities of the final state. Applying the new form of the nonequilibrium free energy to the derivation of solvent reorganization energy, a remarkable feature emerges that the solvent reorganization energies defined for "forward" ET and for "backward" ET are different in general. This is in contrast to the traditional theory of nonequilibrium salvation in which the energies are identical.

The second issue concerned in this work is the implementation of N-PCM model. New subroutines based on the discretizations for both the solute charge and the polarization charge have been written for the Gamess package. The Gamess package has been modified to meet the need for the calculation of the nonequilibrium solvation energy and furthermore the solvent reorganization energy. Through construction of the interaction matrix $\mathbf{D}(\varepsilon_{\rm op})$, based on the PCM technique with the choice of the widely accepted scaling factor of κ=1.2 [27,28], the separation of slow and fast polarization charges on the cavity surface was realized. The newly developed procedure for nonequilibrium solvation energy calculation, N-PCM, was applied to the numerical calculation of $\lambda_{\rm s}$ for two typical Closs-Miller ET systems.

For the semiclassical model of ET, $\lambda_{\rm s}$, $\lambda_{\rm in}$, and $V_{\rm DA}$ play important roles in determining the rate constant. By means of the N-PCM model developed in this work, the solvent reorganization energy was focused on, whereas the inner reorganization energy was evaluated by assuming that only the donor and the acceptor contribute to it. Because of the exclusion of the spacer in the quantum chemical calculation, the inner reorganization energy calculation was performed at a higher level. Making a comparison between the current numerical results and the experimental estimations, the difference for the two model systems is less than 4 kJ/mol. The UHF-SCRF calculation was carried out for $\lambda_{\rm s}$, and the numerical results for this quantity are in perfect agreement with the experimental fittings. In investigating the influence of the scaling factor κ upon the solvent reorganization energy, it was found that $\lambda_{\rm s}$ decreases with the increasing of the scaling factor. The present work confirms that the value of scaling factor, 1.2, which is widely accepted for the equilibrium solvation energy calculation, is also appropriate for the nonequilbrium solvation.

The present study confirms that KT is a powerful tool for the evaluation of electronic coupling. It has advantages such as the easy application and lower cost

DOI:10.1088/1674-0068/21/01/45-54

for computation compared with other approaches. Another function of KT is to approximately determine the position of the transition state of ET by searching for the eigenvalue minimum along a defined reaction coordinate. When KT is applied for the calculation of the electronic coupling, essentially the minimum eigenvalue gap of the frountier MO is used to mimic the transition energy from the ground state to the lowest excited state at the transition geometry. KT is too rough for spectroscopy calculation, but it works for the electronic coupling in ET processes.

V. ACKNOWLEDGMENTS

This work was supported by the National Natural Science Foundation of China (No.20473054 and No.20572073).

[1] J. Cramer and G. Truhlar, Chem. Rev. **99**, 2161 (1999).
[2] J. L. Bredas, D. Beljonne, V. Coropceanu, and J. Cornil, Chem. Rev. **104**, 4971 (2004).
[3] J. Tomasi, B. Mennucci, and R. Cammi, Chem. Rev. **105**, 2999 (2005).
[4] A. J. Klamt, Phys. Chem. **99**, 2224 (1995).
[5] A. Klamt, J. Phys. Chem. **100**, 3349 (1996).
[6] R. A. Marcus, J. Phys. Chem. **98**, 7170 (1994).
[7] P. Vath and M. B. Zimmt, J. Phys. Chem. B **103**, 9130 (1999).
[8] R. L. Blackbourn and J. T. Hupp, J. Phys. Chem. **94**, 1788 (1990).
[9] J. T. Hupp, Y. Dong, R. L. Blackbourn, and H. Lu, J. Phys. Chem. **97**, 3278 (1993).
[10] S. J. Formasinho, L. G. Arnaut, and R. Fausto, Prog. Reaction Kinetics **23**, 11 (1998).
[11] J. R. Miller, L. T. Calcaterra, and G. L. Closs, J. Am. Chem. Soc. **106**, 3047 (1984).
[12] G. L. Closs, L. T. Calcaterra, N. J. Green, K. W. Penfield, and J. R. Miller, J. Phys. Chem. **90**, 3673 (1986).
[13] M. D. Johnson, J. R. Miller, N. S. Green, and G. L. Closs, J. Phys. Chem. **93**, 1173 (1989).
[14] J. R. Miller, B. P. Paulson, R. Bal, and G. L. Closs, J. Phys. Chem. **99**, 6923 (1995).
[15] B. P. Paulson, J. R. Miller, W. X. Gan, and G. Closs, J. Am. Chem. Soc. **127**, 4860 (2005).
[16] M. V. Basilevsky, G. E. Chudinov, I. V. Rostov, Y. P. Liu, and M. D. Newton, THEOCHEM 371, 191 (1996).
[17] M. V. Basilevsky, I. V. Rostov, and M. D. Newton, Chem. Phys. **232**, 189 (1998).
[18] M. V. Vener, I. V. Leontyev, and M. V. Basilevsky, J. Chem. Phys. **119**, 8038 (2003).
[19] I. V. Leontyev, I. V. Tovmash, M. V. Vener, I. V. Rostov, and M. V. Basilevsky, Chem. Phys. **319**, 4 (2005).
[20] Y. R. Mo and J. L. Gao, J. Phys. Chem. B **110**, 2976 (2006).
[21] M. V. Vener, A. V. Tovmash, I. V. Rostov, and M. V. Basilevsky, J. Phys. Chem. B **110**, 14950 (2006).
[22] X. Y. Li and K. X. Fu, J. Comput. Chem. **25**, 500 (2004).
[23] K. X. Fu, Q. Zhu, X. Y. Li, Z. Gong, J. Y. Ma, and R. X. He, J. Comput. Chem. **27**, 368 (2006).
[24] X. Y. Li and K. X. Fu, J. Theor. Comput. Chem. **4**, 907 (2005).
[25] K. X. Fu, X. Y. Li, Q. Zhu, Z. Gong, S. Z. Lu, and Z. M. Bao, THEOCHEM **715**, 157 (2005).
[26] K. X. Fu, Y. Huang, and X. Y. Li, J. Phys. Chem. B **110**, 10088 (2006).
[27] S. Miertus, E. Scrocco, and Tomasi, Chem. Phys. **55**, 117 (1981).
[28] J. Tomasi and M. Persico, Chem. Rev. **94**, 2027 (1994).
[29] V. Barone and M. Cossi, J. Phys. Chem. A **102**, 1995 (1998).
[30] E. Cances, B. Mennucci, and J. Tomasi, J. Chem. Phys. **107**, 3032 (1997).
[31] M. W. Schmidt, K. K. Baldridge, J. A. Boatz, S. T. Elbert, M. S. Gordon, J. H. Jensen, S. Koseki, N. Matsunaga, K. A. Nguyen, S. J. Su, T. L. Windus, M. Dupuis, and J. A. Montgomery, J. Comput. Chem. **14**, 1347 (1993).
[32] H. Li and J. H. Jensen, J. Comput. Chem. **25**, 1449 (2004).
[33] J. D. Jackson, *Classical Electrodynamics*, 3rd Ed., New York: John Wiley & sons, (1999).
[34] R. A. Marcus, J. Chem. Phys. **24**, 979 (1956).
[35] R. A. Marcus, J. Chem. Phys. **38**, 1858 (1963).
[36] Y. P. Liu and M. D. Newton, J. Phys. Chem. **98**, 7162 (1994).
[37] M. Cossi and V. Barone, J. Phys. Chem. A **104**, 10614 (2000).
[38] R. C. Dougherty, J. Chem. Phys. **106**, 2621 (1997).
[39] X. Y. Li and F. C. He, J. Comput. Chem. **20**, 597 (1999).
[40] A. Farazdel, M. Dupuis, E. Clementi, and A. Aviram, J. Am. Chem. Soc. **112**, 4206 (1990).
[41] K. Kumar, I. V. Kurnikov, D. N. Beratan, D. H. Waldeck, and M. B. Zimmt, J. Phys. Chem. A **102**, 5529 (1998).
[42] I. V. Kurnikov, L. D. Zusman, M. G. Kurnikova, R. S. Farid, and D. N. Beratan, J. Am. Chem. Soc. **119**, 5690 (1997).
[43] P. Siddarth and R. A. Marcus, J. Phys. Chem. **94**, 2985 (1990).
[44] S. Z. Lu, X. Y. Li, and J. F. Liu, J. Phys. Chem. A **108**, 4125 (2004).
[45] X. Y. Li, X. S. Tang, and F. C. He, Chem. Phys. **248**, 137 (1999).
[46] M. Cossi, V. Barone, R. Cammi, and J. Tomasi, Chem. Phys. Lett. **255**, 327 (1996).
[47] M. Cossi, B. Mennucci, and R. Cammi, J. Comput. Chem. **17**, 57 (1996).

APPENDIX A:

When the solute charge distribution undergoes a fast change from ρ_1 to ρ_2, the solvent will respond to $\Delta\rho$, with some response modes retarded. If both the atomic and the orientational modes lag, the case is just what was illustrated above, and the problem becomes a mat-

DOI:10.1088/1674-0068/21/01/45-54

ter of electrostatics. Without loss of generality, assume a solvation state to be of a total electric potential ϕ_2, which generally does not equilibrate with the solute charge density ρ_2. This generalized nonequilibrium state is denoted as [ρ_2,ϕ_2] (note that the equilibrium is just a special case of the nonequilibrium). Here we show how to deduce the nonequilibrium free energy for this kind of state, in particular, within the framework of thermodynamics. For this purpose, we consider a constraint equilibrium that is mediated by an external field. This model is, however, completely general, therefore leading to a general expression for the nonequilibrium free energy.

It is understood that, for the nonequilibrium state [ρ_2,ϕ_2], the potential deviates from the equilibrium potential $\phi_2^{\rm eq}$ by an amount of ϕ', i.e.

$$\phi_2 = \phi_2^{\rm eq} + \phi' \tag{A1}$$

In a fast process, the polarization of the solvent partly or completely lags. Therefore, it is easy to realize that such a process is thermodynamically irreversible, and an appropriate thermodynamically reversible pathway should be designed to integrate the free energy change for this fast process. As illustrated in Figure A1, we imagine a proper charge assembly of ρ' outside the solute-solvent system which produces the very potential ϕ' within the system region, so that the system under concern has a potential superposed of $\phi_2^{\rm eq}$ and ϕ'. Since $\phi_2^{\rm eq}$ equilibrates with ρ_2, the system can be charged in a linear fashion,

$$\rho^\alpha = \alpha\rho_2, \quad \phi^\alpha = \alpha\phi_2^{\rm eq}, \quad (\alpha = 0-1) \tag{A2}$$

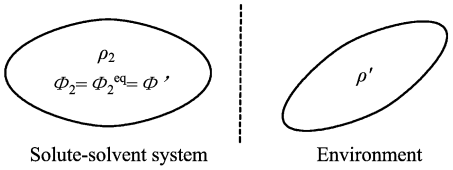

FIG. A1 Constraint equilibrium by an external electric field. $\phi_2^{\rm eq}$ equilibrates with ρ_2 while ρ' is responsible for ϕ'within the system region.

On the other hand, we allow additional free charges to accumulate in the environment region and the potential within the system region to vary accordingly, i.e.

$$\rho^\beta = \beta\rho', \quad \phi^\beta = \beta\phi', \quad (\beta = 0-1) \tag{A3}$$

Both α and β are the charging fractions. This way, the charge assemblies, ρ_2 and ρ', produce the total electrostatic potential ϕ_2 in the system region as shown in Eq.(A1). It should be emphasized here that, although ρ' is responsible for ϕ', the charging work needed for collecting ρ' has nothing to do with the energy exchange between the system and the environment, simply because ρ' occupies the environment region. Therefore, the reversible work done in charging the system is given by

$$\delta W = \int (\phi^\alpha + \phi^\beta)\delta\rho^\alpha {\rm d}V \tag{A4}$$

It is legitimate to assume a synchronous charging process, i.e., α=β, so that Eq.(A4) becomes

$$\delta W = \int \alpha(\phi_2^{\rm eq} + \phi')\delta\rho^\alpha {\rm d}V \tag{A5}$$

The reversible work needed for charging the solute-solvent system from the initial state $[\rho = 0, \phi = 0]$ to the final state $[\rho_2, \Phi_2]$ is thus given by

$$W = \int_V {\rm d}V \int_0^1 \alpha(\phi_2^{\rm eq} + \phi')\frac{\delta\rho^\alpha}{\delta\alpha}{\rm d}\alpha \tag{A6}$$

The nonequilibrium free energy, which is just the reversible work done in the charging process is of the following generalized form,

$$G_2 = \frac{1}{2}\int_V \rho_2\phi_2 {\rm d}V \tag{A7}$$

It is immediately seen that, for an arbitrary potential ϕ_2, no matter whether it equilibrates with ρ_2 or not, the electrostatic free energy can always be written in a very simple form like Eq.(A7), which is applicable to various processes, ranging from very slow ones with respect to the static dielectric constant $\varepsilon_{\rm s}$ to ultra-fast ones corresponding to the optical dielectric constant $\varepsilon_{\rm op}$ of the solvent. Two specific kinds of processes are worth noticing here. By setting ρ'=0 in the above derivation, one obtains the equilibrium free energy corresponding to ρ_2. Setting ϕ_2=$\phi_2^{\rm non}$ in Eq.(A7), with $\phi_2^{\rm non}$ being the nonequilibrium potential composed of $\phi_1^{\rm eq}$ and the potential $\Delta\phi_{\rm op}$ due to $\Delta\rho$ in the hypothetical medium of $\varepsilon_{\rm op}$, we obtain the nonequilibrium free energy for nonequilibrium solvation

$$G_2^{\rm non} = \frac{1}{2}\int_V \rho_2\phi_2^{\rm non} {\rm d}V \tag{A8}$$

DOI:10.1088/1674-0068/21/01/45-54